BOOK OF ABSTRACTS

International Conference on Physics of Light–Matter Coupling in Nanostructures and Nanophotonics

PLMCN 2026

Chairman
Alexey Kavokin — Mediterranean Institute of Fundamental Physics (MIFP)

Co-Chairman
Valentyn Volkov — CTO at XPANCEO

Program Committee Chairman
Aldo Di Carlo — Università degli Studi di Roma Tor Vergata

Yerevan, Armenia
12–15 April 2026
Quantum College

MIFP — Mediterranean Institute of Fundamental Physics

Optically Induced Coulomb Blockade for an Efficient Single-Photon Emission

A. Galimov, M. Rakhlin, Yu. Serov, G. Klimko, M. Kulagina, Yu. Zadiranov and A. Toropov*
Ioffe Institute, 26 Polytekhnicheskaya str., St. Petersburg, 194021, Russia

* Corresponding author: galimov@mail.ioffe.ru

Single-photon sources based on semiconductor quantum dots (QDs) have emerged as an excellent platform for high-efficiency quantum light generation. To date, impressive source efficiencies have been demonstrated using open microcavities [1]. However, such systems require complete vibration isolation and nanometer-precision alignment, which hinders their commercial scalability. In contrast, monolithic sources offer inherent stability. Among them, elliptical micropillars currently achieve the highest reported end-to-end efficiency, reaching 28% [2]. Further improving this efficiency requires full charge-state stabilization of the emitting QD. The most effective technique so far utilizes the Coulomb blockade effect within a doped p-n junction microcavity [3]. Implementing this method is exceptionally challenging, as it demands the fabrication of a high-Q microresonator with a heavily doped active region—a process that introduces significant free-carrier absorption at the QD emission wavelength. In this paper, we present a simpler alternative method for implementing Coulomb blockade in QDs, which enabled us to increase the single-photon emission efficiency in elliptical micropillars to 34%

The single-photon source is an elliptical micropillar containing self-organized InAs/GaAs QDs sandwiched between a bottom (30 pairs) and a top (18 pairs) distributed Bragg reflector [4]. The reactive ion etching method was optimized to obtain strictly vertical sidewalls with minimal roughness. The asymmetry of the resonator induced a polarization degree of 86% for the single-photon emission, which significantly reduced the losses associated with cross-polarization filtering during resonant excitation. Controlling the QD charge state was achieved directly during epitaxial growth by incorporating a p-n-p doping profile into the microcavity [5]. This profile features a thin n-type GaAs layer placed at a predetermined distance from the QD layer. By varying the doping concentration of this n-layer and its separation from the QDs, we can control the relative alignment of the Fermi level with the QD ground-state energy. This enables the fabrication of structures with a predominant population of positively charged, negatively charged, or neutral QDs. A model based on an analytical solution of the Poisson equation shows good agreement with the experimental data. In addition to the main resonant excitation, weak optical illumination with a laser energy above the GaAs bandgap is used. This illumination lowers the potential barrier in the p-n-p structure, allowing fine-tuning of the QD energy level relative to the Fermi level. Once the Fermi level crosses the ground-state energy of the QD, a Coulomb-blockade regime is established within an energy range of about 20 meV.

In this work, we used a QD in a singly hole-charged state as the single-photon source. With Coulomb blockade, we achieved stabilization of this state with a fidelity up to 97%. The optical power required for stabilization was only about 1 pW, thereby preserving the high-quality single-photon emission characteristics under resonant excitation. For a π-pulse excitation condition, the stabilized source exhibits a single-photon intensity of 26.4 MHz at a laser repetition rate of 78.3 MHz. The corresponding single-photon emission efficiency into a single-mode fiber is 34%, which ranks among the highest values reported for monolithic sources. The generated single photons show a purity of 96.3% [$g^{(2)}(0) = 0.037$] and an indistinguishability of 94%.

The work was supported by Rosatom in the framework of the Roadmap for Quantum computing (Contract №. 868/1734-D dated 22 September 2025)

References

[1] X. Ding, Y.-P. Guo, M.-C. Xu *et al*., Nat. Photon. **19**, 387–391 (2025)
[2] H. Wang, Y.-M. He, T.-H. Chung *et al*., Nat. Photon. **13**, 770–775. (2019).
[3] R. Warburton, B. Miller, C. Dürr *et al.*, Phys. Rev. B **58**, 16221 (1998).
[4] A. Galimov, M. Bobrov, M. Rakhlin *et al*., Nanomaterials, **13**, 9 (2023).
[5] A. Galimov, Yu. Serov, M. Rakhkin *et al*., Jetp Lett., **121**, 5 (2025).

Multi-Quantum-Dot Systems in Nanowires

Nika Akopian[a]
DTU Electro, Technical University of Denmark

Semiconductor quantum dots are leading sources of bright, indistinguishable single and entangled photons, making them strong candidates for quantum photonic devices. This work presents two new approaches for integrating multiple deterministically grown quantum dots with excellent optical properties in a single nanowire.

In the first approach, we introduce, for the first time, AlGaAs nanowires as a universal host platform for GaAs, InGaAs, and InAs quantum dots. In the second approach, we develop and demonstrate, for the first time, the deterministic growth of optically active crystal-phase quantum dots emitting single photons.

Synchronization of polariton condensates in aperiodic Penrose tiling

S. Alyatkin[a*], H. Sigurðsson[b], Y.V. Kartashov[a,c], K.A. Sitnik[a], J.D. Töpfer[a], P.G. Lagoudakis[a]

[a] *Hybrid Photonics Laboratory, Skolkovo Institute of Science and Technology, Moscow, Russia*

[b] *Faculty of Physics, University of Warsaw, Warsaw, Poland*

[c] *Institute of Spectroscopy of Russian Academy of Sciences, Moscow, Troitsk, Russia*

* Corresponding author: S.Alyatkin@skoltech.ru

In this work [1], we realize and investigate quasiperiodic arrays of coherently coupled exciton-polariton condensates. Using a reflective spatial light modulator to shape nonresonant laser radiation, we imprint a reconfigurable Penrose tiling potential onto a planar GaAs-based microcavity. The emergence of long-range order is directly observed via the polariton photoluminescence, which exhibits in reciprocal space multiple sharp Bragg peaks with the characteristic 10-fold rotational symmetry of the Penrose lattice. Long-range phase coherence across the aperiodic array is established by ballistic polariton flows, which mediate coupling between distant sites.

The phase map measurements show that, unlike periodic systems [2], the Penrose aperiodic tiling supports nontrivial relative phase configurations between lattice nodes, arising from its unique local connectivity. Furthermore, we show that the phase locking is density-dependent, underscoring the essential role of nonlinear interactions.

This work provides a first look into a 2D quasicrystalline quantum fluid of light, characterized by long-range ballistic coupling, nonlinearities, and extended coherence. By achieving phase synchronization in a flexible, driven-dissipative polariton system in aperiodic conditions, we gain new insights into coherence formation beyond periodic settings. Our results open several future research avenues: studying the role of excitonic vs. photonic fractions on phase locking, exploring spin textures, and investigation of topological states as a function of potential depth.

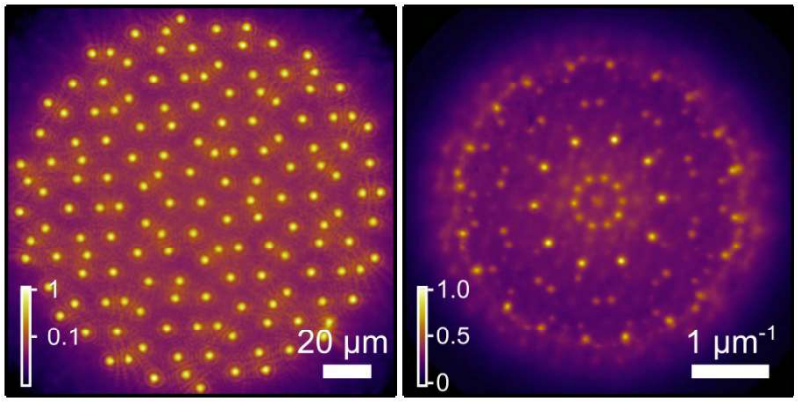

Fig. 1: Experimental evidence of 2D polariton quasicrystal.

References

[1] S. Alyatkin, K. Sitnik, V.K. Daníelsson, Y.V. Kartashov, J.D. Töpfer, H. Sigurðsson, P.G. Lagoudakis, Sci. Adv. **11**, eadz2484 (2025).

[2] S. Alyatkin, H. Sigurðsson, Y.V. Kartashov, I. Gnusov, K. Sitnik, J.D. Töpfer, P.G. Lagoudakis, Appl. Phys. Lett. **124**, 062105 (2024).

Natural Hyperbolic $MoOCl_2$ for Anisotropic Raman Enhancement and Molecular Sensing

Anton Minnekhanov[a*]

[a]*Emerging Technologies Research Center, XPANCEO, Internet City, Emmay Tower, Dubai, United Arab Emirates*

*Corresponding author: minnekhanov@xpanceo.com

Natural hyperbolic media offer a route to deeply subwavelength light confinement and strongly enhanced local photonic density of states, enabling new regimes of light-matter interaction.[1] However, most natural van der Waals hyperbolic crystals operate in the mid-infrared, leaving a long-standing gap in the visible range that is crucial for spectroscopy, biosensing, and integrated nanophotonics.[2] Here we show that $MoOCl_2$, a layered quasi-one-dimensional correlated metal,[3] overcomes this limitation by exhibiting extreme in-plane optical anisotropy in the visible and near-infrared: a metallic response along the crystallographic *a*-axis and a dielectric response along the *b*-axis, which together support in-plane hyperbolic electrodynamics.

Using angle-resolved polarized Raman spectroscopy, we uncover a highly anisotropic vibrational response of $MoOCl_2$ that directly reflects its anisotropic electronic continuum. Raman lineshapes become strongly asymmetric for excitation polarized along the metallic *a*-axis, consistent with pronounced Fano interference between discrete phonons and a continuum of electronic excitations. Beyond lineshape asymmetry, the Raman tensor exhibits excitation-energy-dependent polarization switching, revealing a dispersive redistribution of Raman scattering efficiency between the principal axes. Together, these results provide a compact spectroscopic fingerprint of strong and highly directional light-matter coupling in this natural hyperbolic metal.

We then exploit this anisotropic coupling to demonstrate “Hyperbolic-Enhanced Raman” (HypER) sensing on exfoliated, optically flat $MoOCl_2$ flakes without any lithography or nanoparticle structuring. For a standard dye analyte (Rhodamine 6G), $MoOCl_2$ enables polarization-tunable Raman enhancement factors exceeding 10^7 and detection down to the picomolar level (about 100 pM), while offering an intrinsic “on/off” control via incident polarization alignment with the metallic axis. Importantly, the sensing concept is not limited to dyes: we additionally observe analogous enhancement for other molecular analytes, including doxorubicin, indicating broader applicability for molecular detection relevant to nanophotonics-enabled biosensing.

Our results position $MoOCl_2$ as a simple, air-stable, wafer-compatible platform for visible-range hyperbolic nanophotonics where hyperbolic electrodynamics, anisotropic electronic continua, and Fano-type interference can be harnessed to boost inelastic light scattering and enable polarization-encoded, lithography-free molecular sensing.

References

[1] Poddubny A, Iorsh I, Belov P, and Kivshar Y, Nat. Photonics, 7, 948 (2013)

[2] Basov D, Fogler M, and García De Abajo F, Science, 354, aag1992 (2016)

[3] Venturi G, Mancini A, Melchioni N, Chiodini S, and Ambrosio A, Nat. Commun., 15, 9727 (2024)

Canalized polariton propagation and non-abelian gauge field focusing in perovskite microcavities

Olha Bahrova[a,b,*], Jiahao Ren[c], Feng Jin[c], Hao Zheng[c], Dmitry Solnyshkov[a,d], Cheng-Wei Qiu[e], Guillaume Malpuech[a], and Rui Su[c,f]

[a]*Institut Pascal, PHOTON-N2, Université Clermont Auvergne, CNRS, Clermont INP, F-63000 Clermont-Ferrand, France*

[b]*B. Verkin Institute for Low Temperature Physics and Engineering of the National Academy of Sciences of Ukraine, 47 Nauky Ave., Kharkiv 61103, Ukraine*

[c]*Division of Physics and Applied Physics, School of Physical and Mathematical Sciences, Nanyang Technological University, Singapore, Singapore*

[d]*Institut Universitaire de France (IUF), 75231 Paris, France*

[e]*Department of Electrical and Computer Engineering, National University of Singapore, Singapore, Singapore*

[f]*School of Electrical and Electronic Engineering, Nanyang Technological University, Singapore, Singapore*

* Corresponding author: olha.bahrova@uca.fr

One of the promising advantages of perovskites microcavities is the possibility to host exciton-polaritons at room temperature [1]. In the recent experiment [2], non-equilibrium condensation in CsPbBr3 perovskite microcavity has been achieved under non-resonant pumping. Due to the presence of strong linear birefringence and TE-TM splitting, the dispersion exhibits two tilted Dirac points (DPs) [3] at high wave vectors. The pronounced profile of the dispersion plays a crucial role in the strong redistribution of the intensity in real space. We achieve experimentally coherent polariton beams of different frequency by varying the pump spot size. Thus, we obtain the following regimes of polariton flow according to the shape of the iso-frequency curves (IFCs): hyperbolic (characterized by *effective* negative refractive index), flat and parabolic IFCs, see Fig.1a. In all these cases polariton propagation close to the DPs is strongly collimated. The divergence of the polariton beam calculated from its width determines the collimation factor which takes the biggest value (~20) in the case of flat IFC leading to the pronounced canalization effect, see Fig.1b. From the theoretical side, the above-mentioned reconfigurable polariton canalization effect is reproduced by means of numerical simulations of spinor Gross-Pitaevskii equation (GPE). Moreover, we show that the collimation of polariton beam is strongly enhanced due to the presence of a non-Abelian gauge field [3], which is especially pronounced in the hyperbolic regime.

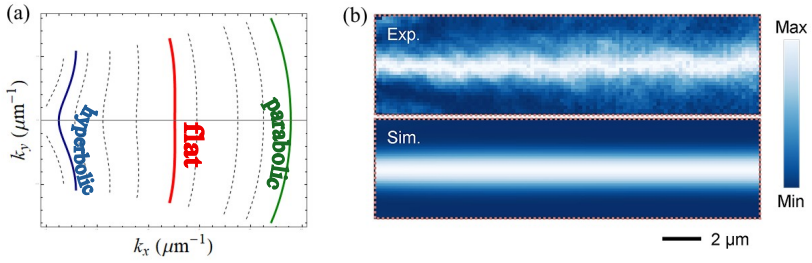

Fig. 1: Canalized polariton flow at flat IFC. (a) Major types of IFCs. (b) Top panel: zoomed experimental real-space image revealing canalized polariton flow toward the +x direction with stable nondiffractive propagation over ~20 µm (normalized for each y coordinate). The bottom panel shows the corresponding theoretical simulation using GPE.

References

[1] R. Su et al. Sci. Adv. **4**, eaau0244(2018) (2018).

[2] J. Ren, O. Bahrova, F. Jin, H. Zheng, D. Solnyshkov, C-W. Qiue, G. Malpuech, R. Su, arXiv:2601.21443 (2026).

[3] H. Terças, H. Flayac, D. Solnyshkov, G. Malpuech, Phys. Rev. Lett. **112**, 066402 (2014).

Dissipative coupling and non-Hermitian effects in polaron-polaritons

M. A. Bastarrachea-Magnani [a*], Diego A. Mendoza [a], Areli J. Vega-Carmona [a], and A. Camacho-Guardian [b]

[a] *Universidad Autónoma Metropolitana-Iztapalapa, Mexico City, Mexico.*

[b] *Instituto de Física, Universidad Nacional Autónoma de México, Mexico City, Mexico.*

* Corresponding author: bastarrachea@xanum.uam.mx

Dissipative coupling refers to the effect in which systems interact with each other through dissipation channels [1]. Recent advances in light-matter systems have opened new avenues to explore non-Hermitian effects arising from dissipative coupling, including level attraction, exceptional points, anomalous dispersion, negative mass, and bound states in the continuum, offering opportunities for propagation engineering, sensing, and more [2]. Exciton-polaritons formed in a microcavity semiconductor serve as a promising platform for studying the interplay between these effects and many-body physics [3-5]. In this work, we present first an analytical study of the parametric effect of dissipative coupling on polariton systems, identifying the conditions for the emergence of non-Hermitian effects [6]. Next, using a quantum field-theoretical formalism [7,8], we extend the analysis to include the interplay between dissipative coupling and polariton Feshbach physics [9] by considering polaron-polaritons, quasiparticles resulting from the interaction between a polariton impurity and a polariton BEC with opposing spin [10]. Finally, the classical limit of the polariton system within a non-Hermitian framework is discussed [11].

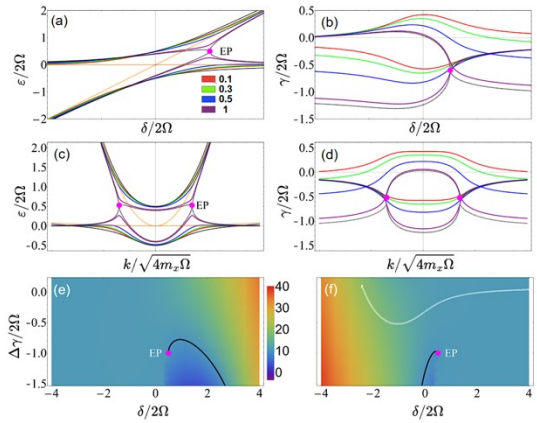

Fig. 1: Real and imaginary parts of polariton branches as a function of detuning (top) and momentum (middle), and polariton effective mass in the relative dissipation and detuning parameter space (bottom).

References

[1] Y.-P. Wang and C.-M. Hu, Journal of Applied Physics 127, 130901 (2020).

[2] M. Harder, B. M. Yao, Y. S. Gui, C.-M. Hu, Journal of Applied Physics 129, 201101 (2021).

[3] C. M. Bender, Reports on Progress in Physics 70, 947 (2007).

[4] S. Dhara, C. Chakraborty, K. M. Goodfellow, L. Qiu, T. A. O'Loughlin, G. W. Wicks, S. Bhattacharjee, and A. N. Vamivakas, Nature Physics 14, 130 (2018).

[5] M. Wurdack, T. Yun, M. Katzer, A. G. Truscott, A. Knorr, M. Selig, E. A. Ostrovskaya, and E. Estrecho, Nature Communications 14, 1026 (2023).

[6] D. Bieganska, M. Pieczarka, C. Schneider, S. Höfling, S. Klembt, M. Syperek, arXiv 2404.14116 (2024).

[7] D. A. Mendoza, A. J. Vega-Carmona, A. Camacho-Guardian, M. A. Bastarrachea-Magnani, arXiv:2512.17833 (2025).

[8] M. A. Bastarrachea-Magnani, A. Camacho-Guardian, and G. M. Bruun, Phys. Rev. Lett. 126, 127405 (2021).

[9] M. A. Bastarrachea-Magnani, J. Thomsen, A. Camacho-Guardian, and G. M. Bruun, Atoms 9 (2021).

[10] N. Takemura, S. Trebaol, M. Wouters, M. T. Portella-Oberli, and B. Deveaud, Nature Physics 10, 500 (2014).

[11] D. A. Mendoza, A. J. Vega-Carmona, A. Camacho-Guardian, M. A. Bastarrachea-Magnani, in preparation.

[12] E.-M. Graefe, M. H¨oning, and H. J. Korsch, Journal of Physics A: Mathematical and Theoretical 43, 075306 (2010).

Ultralong Spin Lifetimes of Optically Oriented Electrons and Holes in Perovskite Semiconductors

Vasilii Belykh[a*]

[a] *Experimentelle Physik 2, Technische Universität Dortmund, 44227 Dortmund, Germany*

* Corresponding author: vasilii.belykh@tu-dortmund.de

Long electron or hole spin lifetimes are essential for quantum technologies based on semiconductor spin qubits. The spin coherence time T_2, which characterizes the unperturbed spin precession about a magnetic field, should allow for execution of 10^4-10^6 qubit operations. At a clock frequency of 100 GHz this requires $T_2 > 10$ μs. Notably, the time T_2 can be extended by decoupling spin qubit from noisy environment to the limit $T_2 = 2T_1$ [1]. Thus, the spin relaxation time T_1 ultimately determines the practical applicability of the spin system.

Many solid-state systems exhibit spin coherence and relaxation times far beyond several μs [2]. Smaller amount exhibit long spin lifetimes at temperatures higher than 1 K. And only a few of these systems allow *optical* spin initialization and manipulation, a prerequisite for high-speed qubit operation. In this talk I will discuss an emerging spintronics platform, perovskite semiconductors, providing optical access to spin states and, as we will see, millisecond-long spin relaxation and coherence times.

Perovskite semiconductors become popular a decade ago as promising materials for photovoltaics, which stimulated much broader studies including investigation of their spin properties. These properties turned out to be similar to those of the most prominent handbook spin systems allowing optical spin manipulation. For a long time the access to the spin coherence and relaxation times in perovskites was obscured by inhomogeneity of the system and limited sensitivity of the experimental techniques. Only recently we have developed a resonant spin inertia technique [3] taking advantage of the pump-probe Faraday rotation and optically detected magnetic resonance (ODMR) techniques, while increasing their sensitivity. This technique enabled access to the millisecond-long spin relaxation times T_1 separately for electrons and holes [4] and excitons [5] in $CsPbBr_3$ and $CsPbI_3$ perovskite nanocrystals.

So far, long spin lifetimes have mainly been observed in strongly confined systems, where the effects of spin –orbit interaction are suppressed: nanocrystals, defects or deep centers embedded in lattice. Perovskites possess unique lattice inversion symmetry, so the most powerful D'yakonov-Perel spin relaxation mechanism related to the spin-orbit interaction turned out to be absent [6]. As a result, we detect ms-long spin relaxation time even in bulk crystals for weakly localized carriers. Moreover, we were able to observe the spin mode locking effect, synchronization of spin precession in electron ensemble, which allowed us to detect ms-long spin coherence times T_2 in bulk $FA_{0.95}Cs_{0.05}PbI_3$ perovskite crystals [7]. Our results highlight perovskites as a unique semiconductor platform for quantum information applications combining optical spin control with exceptionally long spin lifetimes.

References

[1] V. V. Belykh, A. R. Korotneva, and D. R. Yakovlev, Phys. Rev. Lett. 127, 157401 (2021).
[2] P. Stano and D. Loss, Nat. Rev. Phys. 4, 672 (2022).
[3] V. V. Belykh and S. R. Melyakov, Phys. Rev. B 105, 205129 (2022).
[4] V. V. Belykh et al., arXiv:2603.03038 (2026).
[5] V. V. Belykh et al., Nano Lett. 22, 4583 (2022).
[6] N. E. Kopteva et al., Adv. Sci. 12, 2416782 (2025).
[7] S. R. Meliakov et al., arXiv:2601.20768 (2026).

Modeling of phonon-mediated relaxation dynamics towards polariton lasing in microcavity with an arbitrary 2D potential landscape

Oleg Egorov*, Rouziwanguli Wushouer and Ulf Peschel
Institute of Condensed Matter Theory and Optics, Friedrich Schiller University of Jena, Max-Wien-Platz 1, 07743 Jena, Germany

* Corresponding author: oleg.egorov@uni-jena.de

We developed a theoretical approach for simulating collective nonlinear dynamics of exciton-polaritons, considering interaction of excitons with acoustic phonons beyond Fermi's Golden Rule. Formed by the strong light-matter coupling in semiconductor microcavities, exciton-polaritons exhibit fascinating collective phenomena such as nonequilibrium Bose-Einstein condensation [1], superfluidity and polariton lasing [2]. In this contribution, we discuss a model that encompasses the scattering dynamics of exciton-polaritons with acoustic phonons, describing the collective motion within an arbitrary 2D potential landscape [3]. We start from a well-established approach [1] describing the evolution of quantum well excitons coupled to classical photons in semiconductor microcavities. Then we include the wave equation for evolution of 3D acoustic phonons $P_{ph}(x,y,z)$ interacting with 2D excitons of the quantum well (of material density ρ and width d)

$$\partial_t^2 P_{ph}(x,y,z) = v_{ph}^2\left(\partial_x^2+\partial_y^2+\partial_z^2\right)P_{ph}(x,y,z) - \frac{\alpha_0}{\rho d}\left(\partial_x^2+\partial_y^2\right)|\varphi_e(x,y)|^2 f(z),$$

where $f(z)$ describes the quantum well localization function. The excitons interact with acoustic phonons via longitudinal acoustic deformation potential [4] which is accounted by the term $\sim\alpha_0\, P_{ph}(x,y,0)\varphi_e(x,y)$ in the respective differential equation for evolution of exciton collective wave-function $\varphi_e(x,y)$. The initial phonon distribution corresponds to the thermal equilibrium with a well-defined temperature (T).

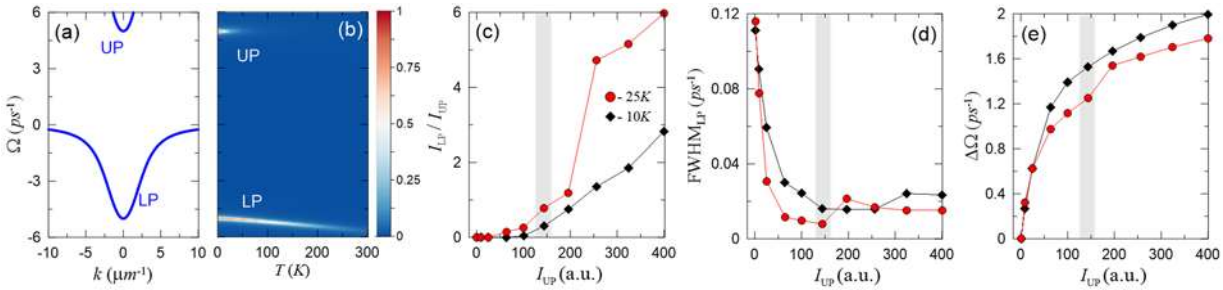

Fig. 1: (a) Dispersion relation shows lower (LP) and upper (UP) polariton branches. (b) Calculated photoluminescence spectra vs. lattice temperatures (T). (c) Intensity of the LP branch vs. incoherent pumping of the UP branch. (d) Linewidth of the LP radiation vs. the pump. (e) Frequency shift vs. the pump.

As a first proof, we calculated photoluminescence and the corresponding spectral response of the lower (LP) and upper polariton (UP) branches as a function of the lattice temperature (see Figs. 1 (a) and 1 (b)). Due to relaxation dynamics, we observe a strong imbalance between the populations of the two branches in favor of the LP branch. Second, to demonstrate the capability of the proposed approach to simulate spontaneous coherence building, we calculated radiation from the ground state (LP) under incoherent pumping in the vicinity of the UP branch. The observed threshold behavior of the input -output characteristic (Fig 1(c)) together with linewidth narrowing at stronger pumping (Fig 1(d)) are typical signatures of polariton lasing. Furthermore, the approach naturally reproduces the frequency blueshift of the radiation know from experiments [1,2].

We note that the model above is suitable for simulations of both relaxation dynamics and polariton lasing of the exciton-polaritons in an arbitrary potential landscape [3] under incoherent pumping conditions.

References

[1] J. Kasprzak *et al*., Nature (London) **443**, 409 (2006).
[2] I. Carusotto and C. Ciuti, Rev. of Mod. Phys. **85**, 299 (2013).
[3] C. Schneider *et. al.*, Rep. Prog. Phys. **80**, 016503 (2017).
[4] W. A. Harrison, Solid State Theory, Dover Publications (1970).

Smart Ports and Safe Borders: The Economic and Environmental Impact of Muon-Based Inspection

Giuseppe Eramo

Faculty of Science in Economics Global Markets and Digital Innovation, University Niccolò Cusano, 00166 Rome, Italy

* Corresponding author: Giuseppe Eramo@unicusano.it

Efficient and reliable inspection of cargo containers remains a structural challenge for modern seaports, where growing commercial flows must coexist with stringent security requirements. Conventional X-ray and gamma-ray Non-Intrusive Inspection (NII) systems, though widely deployed, suffer from inherent limitations: high operational costs, radioprotection constraints, limited penetration in dense cargo, and the inability to scale beyond single-container inspection.

This study presents a quantitative assessment of a next-generation inspection paradigm based on Muon Scattering Tomography (MST), using large-area Resistive Plate Chambers (RPCs) and sub-100 ps Time-of-Flight (ToF) momentum tagging. Through physics-based simulations, port-workflow reconstructions, and techno-economic modelling calibrated on European terminal data, we compare MST with the X-ray baseline.

Results indicate that MST can reduce inspection-cycle time by 60–80% by enabling parallel scanning of 4-5 containers, eliminating radiological delays, and lowering secondary-inspection rates. The economic model predicts €8–12 million annual savings for a medium-size terminal, driven by reduced crane occupancy, diminished dwell time, and lower radioprotection overheads. Environmentally, MST decreases energy consumption and embedded carbon, yielding an estimated 90-tonne annual CO_2e reduction for a 30,000-container flow.

While these findings require validation in real port environments, the combined evidence suggests that MST constitutes a structurally different inspection regime—passive, scalable, and compatible with smart-port logistics. As European ports pursue digitalization and Green Deal targets, MST emerges as a promising pathway toward high-throughput, low-carbon, and security-enhanced border management.

Introduction

Global maritime trade has undergone unprecedented growth over the past decade, with more than 90% of global goods transported in sealed cargo containers according to WTO and WCO estimates [1]. As seaports evolve into increasingly automated and digitally integrated infrastructures, the tension between accelerating commercial throughput and maintaining high levels of border security has become sharper. Customs agencies must detect a widening range of threats-from nuclear materials to illicit goods—while ensuring that inspection processes do not slow down port operations or compromise the competitiveness of national logistics systems.

Traditional Non-Intrusive Inspection systems based on X-ray and gamma-ray technologies remain indispensable tools within this framework. Yet their limitations have been repeatedly highlighted in international assessments [2–5]. Radiographic systems require substantial radiation shielding, operate under strict safety margins, and struggle to penetrate dense or shielded cargo. Their ability to discriminate materials based on atomic composition is limited, particularly in high-Z regimes. Moreover, most current systems are geometrically constrained to inspect one container at a time, a restriction that inherently caps throughput and creates operational bottlenecks in large commercial ports. The consequence is a structural mismatch between inspection capacity and the growing volume of containerized trade.

Muon Scattering Tomography offers a promising complementary approach to bridge this gap. Unlike radiographic systems, MST relies on cosmic-ray muons—a naturally occurring, harmless and deeply

penetrating radiation source present uniformly across the Earth's surface. When muons traverse matter, they undergo multiple Coulomb scattering, an effect governed by the atomic number and radiation length of the material they cross [5,8]. This physical principle gives MST a unique capability: it can probe dense or shielded cargo that conventional radiography cannot reliably image, while remaining completely safe for operators and the environment. As the United Nations has emphasized, such non-ionizing inspection methods are aligned with global sustainability and safety requirements for next-generation border control [3,4].

Over the past fifteen years, several MST prototypes have been developed using a variety of tracking technologies, including drift tubes, scintillator panels, GEM chambers, Micromegas detectors, and Resistive Plate Chambers (RPCs). Projects such as the Decision Sciences MMPDS (USA), the INFN MUON PORTAL (Italy), CRIPT (Canada), and MST components within EU-funded initiatives like C-BORD and SilentBorder have significantly advanced the field. However, all have faced two critical constraints that limit their operational maturity at seaport scale. First, the vast majority rely on average sea-level muon momentum spectra because they cannot measure the momentum of each muon individually. Since scattering angles depend strongly on particle momentum, this leads to systematic uncertainties and limited Z-discrimination capability, a limitation summarized clearly in recent reviews by Bonechi et al. [8-9]. Second, most detectors feature geometries optimized for single-container inspection, making large-scale deployment challenging in high-throughput environments.

Recent technological developments fundamentally shift this landscape. RPCs, originally developed for large-area cosmic-ray experiments such as ARGO-YBJ [17], now offer sub-millimeter spatial resolution and timing precision in the 50–100 ps range when employed in multigap configurations (MRPCs). Such timing accuracy is sufficient to measure the velocity of sub-GeV muons through time-of-flight (ToF) techniques, enabling event-by-event momentum estimation—an innovation that directly addresses the primary limitation of previous MST systems. For energies below ~700 MeV, ToF-based momentum reconstruction provides the missing information required to correctly deconvolve scattering distributions, allowing for true Z-sensitive imaging even in the presence of thick shielding.

Equally transformative is the feasibility of constructing large-area RPC-based tracking systems with industrial scalability. Modular chamber designs with dimensions tailored to cover standard 12-m containers—approximately 2.8×1.1 m² for longitudinal modules and 2.0×1.1 m² for transversal ones-enable full container-width coverage without blind regions. The industrial maturity of RPC technology, proven in high-energy physics installations exceeding 7,000 m², allows the fabrication of large detector planes capable of supporting multi-container tomography. When arranged in stacked configurations above and below container lanes, such systems can exploit existing harbor crane infrastructure to perform parallel scanning of multiple containers, drastically reducing inspection time and enhancing operational throughput.

These developments are complemented by advances in data processing and reconstruction. Machine learning techniques - including convolutional neural networks, graph-based architectures, and physics-informed models-are increasingly used to extract scattering features, enhance angular resolution, and accelerate tomographic reconstruction [13-15]. Combined with modern simulation pipelines based on Geant4, these methods enable realistic training scenarios and robust performance in operational environments. Furthermore, the integration of MST systems within broader smart-port architectures—featuring IoT devices, digital twins, and automated logistics-aligns with current trends in port digitalization and EU strategies for secure and efficient trade.

The environmental and regulatory context also plays a crucial role. With transport representing roughly 25% of EU greenhouse gas emissions [15-16], passive inspection systems based on cosmic muons offer a sustainable alternative to energy-intensive radiographic technologies. Simultaneously, compliance with GDPR and the newly adopted AI Act [13-14] is essential for inspection systems classified as high-risk. MST aligns

naturally with these frameworks: it operates without ionizing radiation, generates inherently anonymous physics data, and can be embedded within secure digital workflows for customs risk analysis.

In summary, recent progress in detector engineering, timing electronics, simulation, and computational reconstruction places MST on the threshold of operational readiness. For the first time, the combination of event-by-event momentum measurement, large-area industrialized RPC systems, scalable parallel scanning, and AI-enhanced reconstruction creates the conditions for a practical, deployable technology capable of addressing modern seaport inspection needs. This article examines the economic, operational, and environmental impacts of adopting such advanced MST systems in European ports, using the Port of Civitavecchia as a representative case. By situating MST within the broader evolution toward smart, secure, and sustainable port ecosystems, we evaluate its potential to reshape the landscape of cargo inspection and border management.

Figure 1 – Conceptual comparison between conventional X-ray Non-Intrusive Inspection (left) and Muon Scattering Tomography (right).

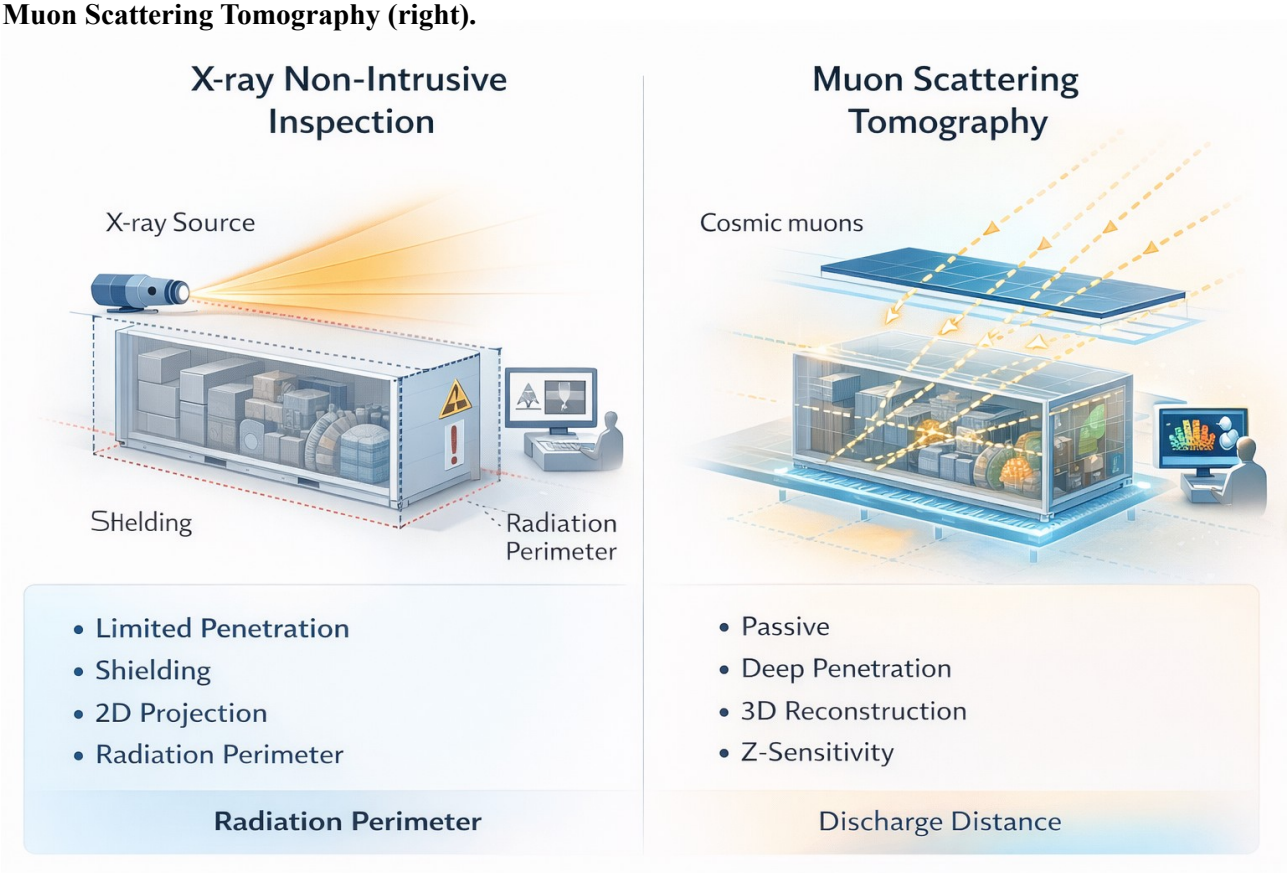

Giant optical anisotropy in van der Waals materials: from magnetic excitons to hyperbolic materials

Georgy Ermolaev[a*]

[a] *Emerging Technologies Research Center, XPANCEO, Internet City, Emmay Tower, Dubai, United Arab Emirates*

* Corresponding author: ermolaev-georgy@xpanceo.com

The quest for the next-generation photonic architectures is fundamentally dependent on the discovery and control of materials exhibiting giant optical anisotropy [1]. Van der Waals (vdW) materials have emerged as a revolutionary platform for this endeavor, offering strong light-matter interactions [2]. However, an experimental challenge has existed in quantifying the full dielectric tensor for these low-symmetry crystals. This work presents a comprehensive determination of these fundamental properties, achieved by applying spectroscopic ellipsometry and Mueller matrix measurements. Our findings reveal new physical regimes, tracing a narrative from magnetically-induced resonances [3,4] to natural hyperbolicity [5].

This exploration begins with magnetic excitons, for which we demonstrate that the interplay of dimensionality, electronic correlations, and magnetism in vdW crystals is a powerful tool for engineering optical anisotropy. For example, we establish that short-range magnetic correlations can stabilize excitons even in bulk, non-magnetic phases of $CrCl_3$ [3] and CrSBr [4]. Moreover, we show that $CrCl_3$ has a record-breaking exciton binding energy of 1.64 eV, an order of magnitude larger than that of typical semiconductors, which we attribute to quasi-2D confinement and robust magnetic correlations that persist at room temperature [3]. In CrSBr, we observe a giant exciton oscillator strength that fundamentally defies established scaling dependencies, as predicted by the Arrhenius law [4]. This anomalous behavior, originating from the 1D electron-hole wavefunction overlap, generates a giant in-plane birefringence of $\Delta n \approx 1.5$ near the exciton resonance [4].

We then push this investigation to the most extreme form of anisotropy: natural hyperbolocity. This exotic state, in which the dielectric tensor components have opposite signs along orthogonal axes, is a primary goal of nanophotonics but has been largely restricted to the mid-IR. We report the first direct experimental determination of the full dielectric tensor of $MoOCl_2$, establishing it as a natural, broadband hyperbolic material for the technologically critical visible and near-infrared spectrum [5]. As a result, our work demonstrates a materials-centric approach using an advanced ellipsometry configuration as a powerful path to unlock novel regimes of light-matter interaction for next-generation nanophotonics.

References

[1] G. Ermolaev et al., Nature Communications, 12, 854 (2021).
[2] A. Slavich, G. Ermolaev et al., Light: Science & Applications, 13, 68 (2024)
[3] G. Ermolaev et al., arXiv:2505.00920 (2025).
[4] G. Ermolaev et al., arXiv:2509.18866 (2025).
[5] G. Ermolaev et al., arXiv:2512.06495 (2025).

Observation of 2D Kardar-Parisi-Zhang universal scaling

Simon Widmann[a], Siddhartha Dam[a*], Johannes Düreth[a], Christian G. Mayer[a], Romain Daviet[b], Carl Philipp Zelle[b], David Laibacher[a], Monika Emmerling[a], Martin Kamp[a], Sebastian Diehl[b], Simon Betzold[a], Sebastian Klembt[a], Sven Höfling[a*]

[a]. *Technische Physik and Würzburg-Dresden Cluster of Excellence ct.qmat, Universität Würzburg, Am Hubland, Würzburg, 97074, Germany.*

[b]. *Institute for Theoretical Physics, University of Cologne, Zülpicher Strasse 77, Cologne, 50937, Germany*

* Corresponding authors: siddhartha.dam@uni-wuerzburg.de; sven.hoefling@uni-wuerzburg.de

Universality provides a powerful framework for grouping systems with different microscopic details into common macroscopic behaviors. Here, we present experimental evidence of two-dimensional Kardar-Parisi-Zhang (KPZ) [1] universal scaling in exciton-polariton condensates.

The KPZ universality class is a paradigmatic example of nonequilibrium physics. While one-dimensional KPZ scaling has been observed in many platforms [2], including exciton-polariton condensates, genuine two-dimensional KPZ behavior can only arise far from equilibrium. Although predicted theoretically [3,4], it has not been experimentally demonstrated so far. Although exciton-polaritons are inherently driven-dissipative, nonequilibrium conditions alone do not guarantee KPZ scaling in two dimensions.

By engineering square and triangular microcavity lattices, we condense polaritons at negative effective-mass states, suppress vortex formation, and realize large, coherent condensates [5]. Using space- and time-resolved interferometry, we measure the first-order coherence function g1(Δr, Δt). Upon rescaling, the data collapse onto the universal 2D KPZ scaling function, yielding critical exponents in quantitative agreement with theory and unambiguously establishing two-dimensional KPZ universality in exciton-polariton condensates.

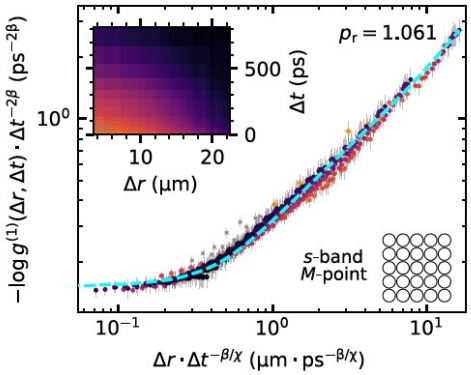

Fig. 1 Scaling collapse of g1(Δr, Δt) obtained for a square lattice onto the theoretically obtained KPZ scaling function

References

[1] M. Kardar, G. Parisi, Y.C. Zhang, Phys. Rev. lett. **56**(9), 889-892 (1986)
[2] Q. Fontaine, et al., Nature **608**(7924), 687-691 (2022)
[3] K. Deligiannis et al., Phys. Rev. Res. **4**, 043207 (2022)
[4] F. Helluin, D. Pinto Dias et al., arXiv:2411.04311v1, (2024)
[5] S. Widmann, Siddhartha Dam et al., arXiv:2506.15521, (2025)

Optical control of nonlinear Hall photocurrents with account of skew scattering in 2D valley semiconductors in the vicinity of a cyclotron resonance

V. N. Ivanova[1,2] *, *V. M. Kovalev*[3,4], *and I. G. Savenko*[1,2]
[1] *Guangdong Technion — Israel Institute of Technology, 241 Daxue Road, Shantou, Guangdong, China, 515063*
[2] *Technion — Israel Institute of Technology, 32000 Haifa, Israel*
[3] *Rzhanov Institute of Semiconductor Physics, Siberian Branch of Russian Academy of Science, Novosibirsk 630090, Russia*
[4] *Novosibirsk State Technical University, Novosibirsk 630073, Russia*
*Corresponding author: ivanovavalerie24@gmail.com

Abstract

We develop a theoretical framework for electromagnetic field-induced transport in two-dimensional (2D) semiconductor thin films, focusing on molybdenum disulfide (MoS_2) as a model material [1]. Using the kinetic equation formalism, we investigate the nonlinear response of the system to an external AC field in the presence of a stationary magnetic field. Importantly, our model incorporates the valley degree of freedom and the trigonal warping of the energy spectrum, which are inherent to MoS_2 monolayers and play a decisive role in their transport properties [2,3].

The study specifically focuses on the microscopic mechanism of asymmetric (skew) scattering on short-range impurities [4]. By calculating the asymmetric part of the scattering probability, we demonstrate how the broken inversion symmetry and valley-specific dynamics contribute to the non-equilibrium distribution of carriers. Our theory predicts the emergence of the photogalvanic effect (PGE), showing that the characteristics of the incident radiation such as frequency and polarization provide a mechanism to control both longitudinal and transverse (Hall) photocurrents. These findings offer a path toward valley-polarized optoelectronics and efficient current manipulation in 2D-based nanophotonic devices.

References

[1] Zhao, Yanchong et al., Origin of Nonlinear Circular Photocurrent in 2D Semiconductor MoS_2. Phys. Rev. Lett. 134, 086201 (2025).

[2] V. M. Kovalev, A. V. Parafilo, O. V. Kibis, and I. G. Savenko, Role of the Coulomb interaction in the valley photogalvanic effect, Phys. Rev. B 109, 245414 (2024).

[3] X. Zhou, et al., Universal classes of disorder scatterings in in-plane anomalous Hall effect, arXiv:2501.02533 (2025).

[4] A. Veneri, A. Ferreira, et al., Extrinsic Orbital Hall Effect: Orbital Skew Scattering and Crossover Between Diffusive and Intrinsic Orbital Transport, arXiv:2408.04492 (2024).

Enigma of Polariton Simulators

Junhui Cao[a] and Alexey Kavokin[a,b*]

[a] *Abrikosov Center for Theoretical Physics, Moscow Institute of Physics and Technology, Dolgoprudny, 141701, Russia*

[b] *School of Science, Westlake university, Shilongshan Road, 18, Hangzhou 310024, China*

* Corresponding author: kavokinalexey@gmail.com

Ultrafast analogue simulators based on arrays of bosonic condensates of exciton-polaritons have been proposed and experimentally demonstrated by Berloff et al, [1]. Their seminal work has been followed by an avalanche of publications which reported on the experimental realization of polariton XY-simulators and proposed their theoretical description, most based on numerical solutions of generalized Gross-Pitaevskii equations [2]. Polariton simulators are so attractive because they offer the advantage of unprecedently fast operation speed. An array of several tens (perhaps hundreds or even thousands) polariton condensates excited by non-resonant optical pumping finds a phase-locked state on a time scale of <100 ps. According to the proposal of Berloff et al, [1] this phase locked state can be mapped to the lowest energy eigen-state of a classical spin Hamiltonian, where the phase of each condensate sets the orientation of the corresponding spin.

Scaling the system up to several thousand spins makes the problem of finding the ground state of an XY-spin Hamiltonian very hard computationally. A simulator able to solve this problem on a time scale of 100 ps would outperform any existing classical computer. Still, several crucial issues are pending satisfactory answer: (1) how the operation time of the proposal polariton simulator scales with the number of condensates in the array? (2) how the fidelity of such a device would depend on the size of the system? (3) what is the range of external parameters (such as the pump power, average distance between the condensates in the array, size of the pump spots etc) where the device is expected to operate as it should?

We present an analytical model of the polariton XY-simulator that answers these important questions. In contrast to previously published theories, we consider a problem of N-coupled polariton condensates using the tools of linear quantum mechanics. We study the formation dynamics of all existing multi-condensate eigen-modes in a system of N coupled polariton condensates. We find eigen-functions of these modes by diagonalising a tight-binding Hamiltonian of the system. Solving analytically Boltzmann type rate equations for each of these modes we derive the threshold pump power needed to trigger the Bose-Einstein condensation. Ranging the modes by the threshold pump power and calculating the formation rates of Bose-Einstein condensates of exciton polaritons in each of them we succeeded obtaining full and comprehensive answers to the key questions (1-3) formulated above. To illustrate our conclusions, we addressed in great detail important particular cases of linear chain and triangular lattice of polariton condensates as well as the case of a random graph.

We are confident that this comprehensive analytical study complemented by numerical calculations performed for several realistic polariton systems is essential not only for the practical development of ultrafast polariton simulators but also for understanding of the underlying physics of interacting bosonic condensates of quasiparticles in a driven-dissipative system.

References

[1] N.G. Berloff et al, *Nature Materials.* **16**, 1120 (2017).

[2] J. D. T¨opfer, et al, *Communications Physics* **3**, 2 (2020).

Quantum vs Quantum Optical Coherence of Polaritons

Fabrice P. LAUSSY

Instituto de Ciencia de Materiales de Madrid ICMM-CSIC, 28049 Madrid, Spain

fabrice.laussy@gmail.com

As a superposition $\alpha|0,1\rangle + \beta|1,0\rangle$ of light and matter, the microcavity polariton [1] seems ideally suited to exhibit quantum effects. Yet, however practical is a mental picture, it might be just this: a practicality disconnected from the more clumsy but less exotic reality. This was illustrated for instance with Mølmer's depiction of "optical coherence" as a convenient fiction [2]. Similarly, within a quantum formalism, polaritons are often more accurately described as product states (not superpositions) of coherent states (not Fock states) [3]:

$$|\psi\rangle = |\alpha\rangle \otimes |\beta\rangle$$

where α and β are the same mathematical quantities in both expressions, two complex numbers following the same equations, but with different interpretations: quantum amplitudes in the former case and classical field of a coherent state in the latter. Such distinctions as well as relationships are crucial for a proper discussion of quantum information processing with polaritons. It is indeed possible to deal with genuinely quantum states of the polariton field, but this may require special efforts to get there, such as exciting them with a quantum source [4], as was indeed demonstrated [5]. Recently, another layer of similar subtlety was added to the cake from quantum resource theory [6], which quantifies how "useful" is a "resource" from given states of a system, e.g., such as entanglement from coupled qubits. For polaritons, this took the form of quantifying so-called "quantum coherence" as a resource from polariton condensates [7-9]. There, a coherent state is regarded as a quantum resource. Quantum coherence is *not* Glauber's quantum optical coherence. One quantifies purity (off-diagonal) while the other quantifies Poissonianity (diagonal elements of the density matrix). In this talk, I will review this emerging trend of the field and challenge its claim as to whether quantum coherence is a way to make polariton more quantum than they typically are.

[1] A. V. Kavokin, J.J. Baumberg, G. Malpuech and F.P. Laussy. Microcavities. Oxford University Press, 2017.

[2] K. Mølmer. Optical coherence: A convenient fiction. Phys. Rev. A, 55:3195, 1997.

[3] L. Dominici *et al.* Ultrafast control and Rabi oscillations of polaritons. Phys. Rev. Lett., 113:226401, 2014.

[4] J. C. López Carreño *et al.* Exciting polaritons with quantum light. Phys. Rev. Lett., 115:196402, 2015.

[5] A. Cuevas *et al.* First observation of the quantized exciton-polariton field and effect of interactions on a single polariton. Science Advances, 4:eaao6814, 2018.

[6] E. Chitambar and G. Gour. Quantum resource theories. Rev. Mod. Phys., 91:025001, 2019.

[7] C. Lüders *et al.* Quantifying quantum coherence in polariton condensates. Phys. Rev. X Quantum, 2:030320, 2021.

[8] Y. Brune *et al.* Quantum coherence of a long-lifetime exciton-polariton condensate. Commun. Mater., 6:123, 2025.

[9] Y. Brune *et al.* Quantum resource theory of lasers. Phys. Rev. Res., 8:013170, 2026.

Low-power topological darkness sensors based on anisotropic reflection

Valeria Maslova[a,b*] and Denis G. Baranov[a]

[a] *Emerging Technologies Research Center, XPANCEO, Internet City, Emmay Tower, Dubai, UAE*

[b] *C.H.O.S.E. (Center for Hybrid and Organic Solar Energy), Electronic Engineering Department, University of Rome Tor Vergata, Via del Politecnico 1, 00118, Rome, Italy*

* Corresponding author: lera.maslova00@gmail.com

Perfect absorption accompanied by phase singularity is an increasingly important phenomenon in light-matter interaction. Despite relatively simple physical origin, it enables elegant and diverse applications, including ultrafast analog computing [1], holography [2], and ultrasensitive molecular detection platforms [3-4]. However, the structural complexity of existing implementations motivates the search for alternative optical systems capable of supporting phase singularities. In addition, the robustness of such systems against noise and imperfections present in real physical environments remains an open question.

In this work, we demonstrated that phase singularities can be realized in reflection from an anisotropic material. We derived the analytical condition required for the emergence of the phase singularity and analyzed its evolution within the system parameter space. Using the proposed platform (Fig. 1(a, b)), we investigated the effect of shot noise on the performance of a refractometric sensor. We developed a realistic ellipsometric model operating near a zero-signal condition with incorporated shot noise model to numerically evaluate the statistical properties of the sensing scheme.

Our analysis revealed two key mechanisms which determine sensor resolution associated with theoretical sensitivity and short noise fluctuations. We presented a method to estimate the achievable resolution and identify the optimal operational regime in which these competing effects are balanced through appropriate adjustment of the angle of incidence for a given sensing problem (Fig. 1(c)).

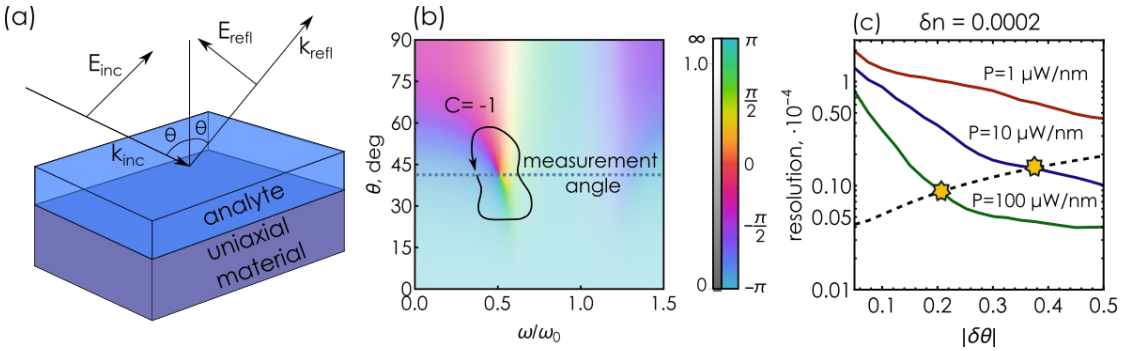

Fig. 1: (a) Sketch of the refractometric sensor under study: a uniaxial absorbing material covered with an optically thick layer of analyte. (b) Plot of the complex-valued ellipsometric response function for the system in (a). (c) Behavior of the sensor's noise-limited (solid lines) and sensitivity-limited (dashed line) resolution with the analyte refractive index shift $\delta n = 0.0002$ for different source powers. The asterisks indicate the optimal incidence angle at which the sensor exhibits the optimal resolution.

These findings demonstrate that topological darkness sensors can operate efficiently even at low illumination power, making them promising candidates for compact and energy-efficient optical devices.

References

[1] Zhu T., et al, Topological optical differentiator, Nature Communications, 2021, vol. 12(1): 680.

[2] Yingwei Wang, et al, Atomically Thin Noble Metal Dichalcogenides for Phase-Regulated Meta-optics, Nano Letters, 2020, vol. 20 (11)

[3] Kravets V. G., et al, Singular phase nano-optics in plasmonic metamaterials for label-free single-molecule detection, Nature materials, 2013, vol. 12(4): 304-309.

[4] Ermolaev G., et al, Topological phase singularities in atomically thin high-refractive-index materials, Nature Communications, 2022, vol. 13(1): 2049.

Flat bands in a chain of coupled laser dimers

Alexey Osipov [a,b,c*], Ivan Savenko[b, a], Sergej Flach[d] and Alexey Yulin[c]
[a] *Technion – Israel Institute of Technology, 32000 Haifa, Israel*
[b] *Department of Physics, Guangdong Technion–Israel Institute of Technology, 241 Daxue Road, Shantou, Guangdong 515063, China*
[c] *Department of Physics, ITMO University, Saint~Petersburg 197101, Russia*
[d] *Institute for Basic Science, Daejeon, Republic of Korea*

* Corresponding author: aleksey.osipov@metalab.ifmo.ru

Flat bands in condensed matter physics are known for hosting peculiar phenomena, including localization of excitations, density of states singularities, and emergence of exotic quantum states [1]. However, flat bands are highly sensitive to perturbations, making their observation challenging and typically requiring fine-tuning or symmetry protection. In our work, we present a novel approach to selectively populate and manipulate flat bands within a driven-dissipative non-Hermitian system: a one-dimensional chain of coupled lasing dimers.

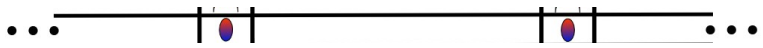

Fig. 1: Schematic illustration of laser dimers consisting to lasers coupling via optical waveguide **A**. The dimers coupled with each other via common perpendicular waveguide **W** forming a chain

We consider active optical resonators coupled via vertical optical waveguides forming laser dimers. The dimers are coupled with each other through a common horizontal waveguide **W**. To be specific, we consider polaritonic Bose-Einstein condensates in microresonators coupled to optical waveguides. Using a coupled-mode approximation, we demonstrate that the synchronization regime of the dimers (in-phase ($\Delta\phi=0$) or antiphase ($\Delta\phi=\pi$) configuration) can be dynamically controlled via in-situ tuning of non-resonant pumping intensity.

Flat bands emerge in linear excitation spectra of the chain of coupled dimers for both in-phase and antiphase dimer configurations. However, they exhibit drastically different behaviors. In the antiphase regime, the flat band corresponds to the dominant mode, manifesting the system as a sequence of non-interacting compact localized states (CLSs) that are uncoupled from the rest of the lattice. In this regime radiation into the horizontal waveguide is suppressed due to the destructive interference. Evidently, flat bands can be clearly observed in the noise response spectra. Moreover, if the pump is switched off after a stable state has formed, the properties of flat bands in the quasi-conservative limit can be studied. In contrast, in-phase synchronized dimers actively emit into the horizontal waveguide **W** leading to phase-locking of dimers in the chain. Finally, we demonstrate pump-controlled phase transitions between these configurations.

Our findings provide a novel perspective on flat bands in non-Hermitian systems, opening avenues to study both conventional linear flat bands and flat bands in the excitation spectra of laser lattices.

References

[1] D. Leykam, A. Andreanov, and S. Flach, Advances in Physics: X 3, 1473052 (2018).

When Nanowires Go Wurtzite: Direct Gaps and Near-Crossover Physics in AlGaAs

Daniele Barettin[a,*]

[a] *eCampus University, Department of Theoretical and Applied Sciences, Novedrate, Italy*

* Corresponding author: daniele.barettin@uniecampus.it

Wurtzite $Al_xGa_{1-x}As$ nanowires are a promising platform for band-gap engineering, quantum photonics, and crystal-phase-based nanostructures. Here I report new results on the band-gap evolution of wurtzite AlGaAs nanowires over an extended Al-composition range, combining photoluminescence measurements, first-principles calculations, and effective modeling.

Macro- and micro-photoluminescence measurements show clear optical emission up to nominal Al contents of x=0.9, extending the experimentally accessible range well beyond previous studies, while no signal is detected for the AlAs end member under the present conditions. The comparison with DFT-HSE calculations shows excellent agreement up to about $x \sim 0.4$, indicating that theory captures the main evolution of the direct gap in the low- and intermediate-Al regime. At higher Al content, the DFT results become systematically larger than the measured optical transition energies and predict the onset of indirect-gap behavior above about $x \approx 0.70$. However, the calculated direct and indirect gaps remain separated by only a few tens of meV in the Al-rich regime, pointing to a near-degenerate crossover region rather than a sharp transition. This provides a natural explanation for the persistence of optical activity in real nanowires up to high Al content, where alloy disorder, local composition fluctuations, and localization effects may sustain radiative emission even as the electronic structure approaches an indirect-gap configuration.

For completeness, Fig. 1 also includes an effective k·p fit of the full experimental dataset up to nominal x=0.9, providing a practical description of the measured gap evolution. Overall, these results further establish wurtzite AlGaAs nanowires as a versatile material platform in which direct-gap behavior, near-crossover physics, and quantum confinement can be tailored within a single system.

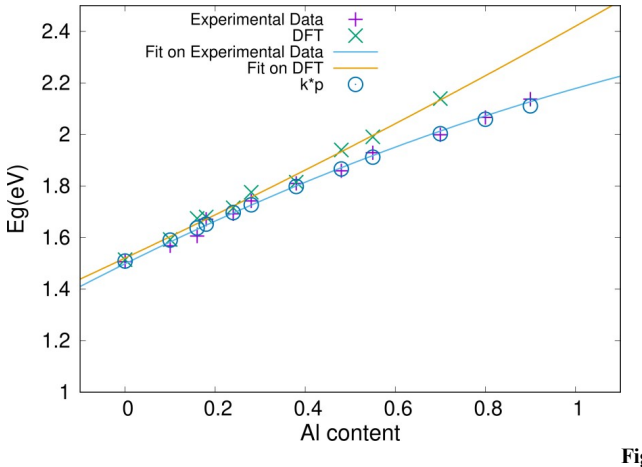

Fig. 1: Experimental gap energies, DFT results, corresponding fits, and effective k·p description for wurtzite $Al_xGa_{1-x}As$ nanowires as a function of nominal Al content.

References

[1] L. Leandro, C. P. Gunnarsson, R. Reznik, K. D. Jöns, I. Shtrom, A. Khrebtov, T. Kasama, V. Zwiller, G. Cirlin, and N. Akopian, *Nanowire Quantum Dots Tuned to Atomic Resonances*, Nano Lett. **18**, 7217–7221 (2018).

[2] D. Barettin, I. V. Shtrom, R. R. Reznik, S. V. Mikushev, G. E. Cirlin, M. Auf der Maur, and N. Akopian, *Direct Band Gap AlGaAs Wurtzite Nanowires*, Nano Lett. **23**, 895–901 (2023).

Scaling up of organic semiconductor nanocomposites for low-temperature-grade energy harvesting: from cell to module

Andrea. Reale[1*]

[1] *Centre for Hybrid and Organic Solar Energy (CHOSE), Department of Electronic Engineering, University of Rome Tor Vergata, via del Politecnico 1, 00133 Rome, Italy*

* Corresponding author: reale@uniroma2.it

Thermoelectric (TE) materials, in the context of recent technological advancements, are regarded as the foremost choice for converting waste heat into electrical energy [1]. Nonetheless, their industrial application is constrained by factors such as high-temperature fabrication processes, the high cost of inorganic TE materials, and their inherent toxicity. In the past decade, composites of organic polymers with carbon-based nanostructures, such as graphene nanoplatelets or carbon nanotubes, have attracted considerable attention as TE materials suitable for energy harvesting applications [2-6].

We successfully developed and characterized a printable TE composite paste based on GNPs and P3HT, tailored for low-temperature energy harvesting applications. By systematically varying the GNP:P3HT ratios and incorporating dopants such as LiTFSI and TBP, we achieved significant improvements in electrical conductivity, Seebeck coefficient, and overall power factor. Comprehensive morphological and Raman analyses revealed that doping not only improved charge carrier mobility and interfacial interactions but also promoted a more uniform and well-ordered composite structure. Among all tested configurations, the GNP:P3HT(LiTFSI+TBP) 1:2 composite exhibited the best performance, attaining a power factor exceeding 1000 nW/mK2 for thin film, marking a substantial leap over undoped counterparts. Pelletized versions of the optimized composite, including TiO2 NP, were used to fabricate a functional TE module, validating the scalability of the material system.

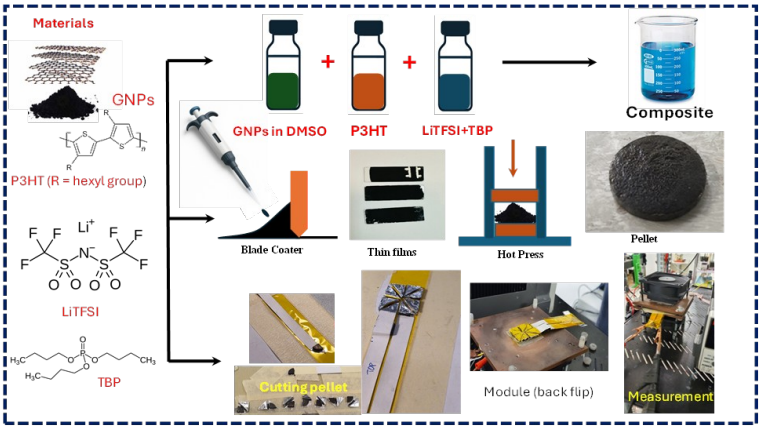

References

[1] C Artini, G Pennelli, P Graziosi, Z Li, N Neophytou, C Melis, L Colombo, et al., Roadmap on thermoelectricity, Nanotechnology 34 (29), 292001, https://doi.org/10.1088/1361-6528/acca88

[2] Saeed Mardi, Marialilia Pea, Andrea Notargiacomo, Narges Yaghoobi Nia, Aldo Di Carlo and Andrea Reale, The Molecular Weight Dependence of Thermoelectric Properties of Poly (3-Hexylthiophene), Materials 2020, 13, 1404; doi:10.3390/ma13061404

[3] Saeed Mardi, Marco Risi Ambrogioni and Andrea Reale, Developing printable thermoelectric materials based on graphene nanoplatelet/ethyl cellulose nanocomposites, 2020 Mater. Res. Express https://doi.org/10.1088/2053-1591/ababc0

[4] Saeed Mardi, Pietro Cataldi, Athanassia Athanassiou, and Andrea Reale, "3D cellulose fiber networks modified by PEDOT:PSS/graphene nanoplatelets for thermoelectric applications", Appl. Phys. Lett. 120, 033102 (2022); doi: 10.1063/5.0075918

[5] Saeed Mardi, Khabib Yusupov, Patricia M. Martinez, Anvar Zakhidov, Alberto Vomiero, Andrea Reale, Enhanced Thermoelectric Properties of Poly(3-hexylthiophene)through the Incorporation of Aligned Carbon Nanotube Forest and Chemical Treatments, American Chemical Society – ACS Omega, DOI: 10.1021/acsomega.0c02663

[6] Graphene-based organic semiconductor composites for low-temperature-grade energy harvesting: From cell to module, Sajid Muhammad , Syzmon Gococ , Marcello Franzini , Simone Galliano, Claudia Barolo, Andrea Reale, Energy Reports 14 (2025) 4006–4014, doi:10.1016/j.egyr.2025.11.020

Optical properties and THz applications of nanocarbons

M.E. Portnoi*

Physics and Astronomy, University of Exeter, Stocker Road, Exeter EX4 4QL, UK

* Corresponding author: m.e.portnoi@exeter.ac.uk

Carbon-based nanostructures are believed to be promising candidates for terahertz (THz) applications [1]. Following our earlier work on narrow-gap carbon nanotubes and graphene nanoribbons [2], as well as graphene bipolar waveguides [3] and double quantum wells [4], we are now considering dipole optical and terahertz transitions in two other types of nanocarbons – carbynes and cyclocarbons.

The technology for synthesizing carbynes (polyyne carbon chains) has rapidly evolved over the last few years, with stable long chains deposited on substrates now a reality [5]. We have recently demonstrated and explained a strong polarization dependence of photoluminescence from highly aligned carbon chains terminated by gold clusters [6]. A prominent feature of long polyyne chains (chains with two alternating non-equal bonds) is the presence of topologically protected mid-gap edge states. For a finite-length chain, the two edge states form an even and odd combination with the energy gap proportional to the edge-state overlap due to tunneling. These split states of different parity support strong dipole transitions. We have shown [7] that for long enough carbyne chains, the energy separation between the HOMO and LUMO molecular orbitals formed by the edge states corresponds to the THz frequency range. There are several other allowed optical transitions in this system that can be used to maintain the inversion of population required for THz lasing. The frequency of THz transitions can be tuned by an external electric field [8].

Another recent achievement in nanocarbon technology is the demonstration of controlled synthesis of cyclocarbons, particularly the cyclocarbon allotropes C_{18} [9] and more recently C_{16} [10]. The properties of cyclocarbons in an external (lateral in the plane of the molecule) electric field differ drastically depending on the parity of the number of dimers in a polyyne ring. This is a direct consequence of breaking the inversion symmetry in a ring consisting of an odd number of dimers, including the famous C_{18}. Our estimates [11] show that adding just one extra carbon dimer to C_{16} is equivalent to placing this molecule in an external magnetic field of over 1000 T. For a polyyne cyclocarbon with an odd number of dimers, because of the absence of inversion symmetry, an experimentally attainable electric field should open a tunable gap between otherwise degenerate states, leading to two states with allowed dipole transitions between them in the THz range. Population inversion can be achieved again using optical pumping.

This work was supported by the EU H2020-MSCA-RISE project CHARTIST (H2020-101007896), EU Horizon Europe MSCA Staff Exchange project HERMES (HE-101236439) and by the UK EPSRC grant EP/Y021339/1.

References

[1] R. R. Hartmann, J. Kono and M. E. Portnoi, Nanotechnology, **25**, 322001 (2014).

[2] R. R. Hartmann, V. A. Saroka and M. E. Portnoi, J. Appl. Phys., **125**, 151607 (2019).

[3] R. R. Hartmann and M. E. Portnoi, Phys. Rev. B, **102**, 155421 (2020).

[4] R. R. Hartmann and M. E. Portnoi, Phys. Rev. A, **102**, 052229 (2020).

[5] S. Kutrovskaya et al., Nano Lett., **20**, 6502 (2020).

[6] A. Kucherik et al., Phys. Rev. Lett. **132**, 056902 (2024).

[7] R. R. Hartmann et al., Physical Review Research, **3**, 033202 (2021).

[8] R. A. Ng, M. E. Portnoi and R. R. Hartmann, Small Structures, **6**, e202500266 (2025)

[9] K. Kaiser et al., Science, **365**, 1299 (2019).

[10] Y. Gao et al., Nature, **623**, 977 (2023).

[11] R. A. Ng, M. E. Portnoi and R. R. Hartmann, Phys. Rev. B, **106**, L041403 (2022).

Polaritons without excitons: the mechanism of lasing in lead halide perovskites

M. Saba[1], A. Simbula, N. Sestu[1], F. Mattana[1], D. Marongiu[1], V. Demontis[1], F. Quochi[1], A. Mura[1], G. Bongiovanni[1]

[1]Dipartimento di Fisica, Università di Cagliari, Italy

Abstract— Lead halide perovskites are well known for their very large optical absorption coefficient in the visible spectrum, enabling thin film solar cells, few hundreds of nanometres in thickness, to fully absorb sunlight. Quantum mechanical unitarity of the absorption process ensures that the reciprocal process, optical emission, has an equally large matrix element and therefore is also very efficient, a feature that is known as reciprocity and that ensures that the best possible solar cell materials are also the best possible light emitting ones.

I will present evidence that light-matter is strong enough to give rise to polariton states, with a distinctive dispersion, even in unpatterned perovskite thin films, without external cavities or light confinement structures. Since correlated electron-hole pairs are the majority optical excitations in 3D hybrid perovskite thin films at room temperature, such polaritons are of a novel kind, not exciton-polaritons, but more appropriately band-edge polaritons. Not having to depend on the stability of bound excitons, band-edge polaritons survive at very large excitation densities.

Ultrafast optical spectroscopy experiments demonstrate that band edge polaritons even undergo Bose-Einstein condensation at the threshold for stimulated emission. Such findings open new avenues for perovskite optoelectronics thanks to the peculiar properties of polaritons: firstly, polariton lasers are potentially thresholdless because they do not require inversion nor optical gain; second, polaritons propagate at large speed in planar waveguides, and may be applied to integrated photonic circuits; third, and most important, polaritons inherit the strong nonlinearities from their matter component, so that efficient quantum gates may be realized.

Perovskite solar modules and panels with advanced surface modification for enhanced power output in ambient conditions

Pavel A. Gostishchev[1], Lev O. Luchnikov[1], Ekaterina A. Ilicheva[1], Andrei P. Morozov[1], Artur R. Ishteev[1], Anna A. Zarudnyaya[1] and Danila S. Saranin[1]

[1]*Laboratory of Advanced Solar Energy (LASE), National University of Science & Technology MISIS, 6 Leninsky Ave., Moscow, 119049, Russia*

Corresponding author: Dr. Danila S. Saranin (saranin.ds@misis.ru)

Perovskite photovoltaics are approaching commercialization, yet deployment at the panel level is still constrained by operational stability in the field and by defect- and ion-driven degradation pathways that intensify under heat, humidity, and electric bias[1]. Here, a scalable fabrication-to-exploitation workflow was demonstrated for terrestrial p-i-n perovskite modules and a prototype panel. Outdoor operation was evaluated by parallel monitoring of an experimental perovskite solar panel and an industrial HJT Si reference during September-November 2025 using a validated protocol with synchronized irradiance and temperature telemetry. Across the accepted measurement runs, the perovskite panel exhibited a clear advantage in specific energy yield under low-irradiance conditions typical for overcast and variable-weather operation (<200 W m^{-2}). In the threshold low-light regime (daily integrated insolation from 1.51×10^{-2} to 1.38×10^{-1} Wh cm^{-2}, with typical levels ≤150 W m^{-2} and short peaks up to ~460 W m^{-2}), the perovskite panel outperformed the silicon analogue, showing gains from ~12% To address durability limitations, two complementary materials approaches were emphasized. First, integration of the layered perovskite $AVA_2FAPb_2I_7$ as an inter-grain heterostructure within $CsFAPbI_3$ reshaped inter-grain energetics and increased chemical robustness against thermal cycling, humidity, and electric fields[2]. The heterostructure suppressed ion migration and inhibited metal/perovskite corrosion; surface-contact studies indicated stabilized iodine/lead states and reduced copper oxidation, consistent with limiting diffusion of reactive species toward electrodes. Second, bulk SAM modification using an asymmetric TPA-Py molecule (triphenylamine donor with pyridine acceptor) introduced strong dipole-driven band bending and reduced non-radiative recombination, while screening ionic-defect transport (activation energy 0.45 eV from PIVTS)[3]. Consequently, open-circuit voltage increased to 1.14 V and efficiency to 21.3%, and thermal lifetime improved markedly: T80 rose from 260 h to >700 h under ISOS-D-2 (85°C). Overall, the results link low-light exploitation advantages with scalable, intrinsic stabilization routes for durable perovskite panels.

The Authors gratefully acknowledge the financial support from Russian Science Foundation project № 22-19-00812-P.

[1] P. Čulík, K. Brooks, C. Momblona, M. Adams, S. Kinge, F. Maréchal, P. J. Dyson, M. K. Nazeeruddin, *ACS Energy Lett.* **2022**, *7*, 3039.

[2] L. O. Luchnikov, E. A. Ilicheva, V. A. Voronov, P. A. Alekseev, M. S. Dunaevskiy, V. Kalinichenko, V. Ivanov, A. Furasova, D. A. Krupanova, E. V. Tekshina, S. A. Kozyukhin, D. S. Muratov, P. K. Sukhorukova, M. I. Voronova, D. S. Saranin, E. I. Terukov, *Appl. Surf. Sci.* **2026**, *716*, 164693.

[3] https://doi.org/10.48550/arXiv.2510.08401

Chiral Light-Matter Coupling and Directional Emission in Glide-Plane Photonic Crystal Waveguides.

Savvas Germanis[a,*], Xuchao Chen[a], Hamidreza Siampour[b], René Dost[a], Dominic J. Hallett[a], Edmund Clarke[c], Pallavi K. Patil[c], Maurice S. Skolnick[a], Luke R. Wilson[a] and Antony M. Fox[a]

[a] *School of Mathematical and Physical Sciences, University of Sheffield, Sheffield, UK*

[b] *School of Mathematics and Physics, Queen's University Belfast, Belfast, UK*

[c] *EPSRC National Epitaxy Facility, University of Sheffield, Sheffield, UK*

* Corresponding author: s.germanis@sheffield.ac.uk

Chiral light-matter interaction provides a powerful mechanism for spin-dependent photon routing and constitutes a central resource for integrated quantum photonics. Glide-plane photonic crystal waveguides offer a nanophotonic platform in which broken mirror symmetry generates locally circularly polarised guided modes, giving rise to spin-momentum locking between quantum dots' spin states and propagating photons [1].

We present experimental investigations of individual InAs quantum dots embedded in the slow-light region of glide-plane waveguides, where both strong Purcell enhancement and high optical chirality can be achieved simultaneously. Spectral tuning of the exciton transition across the slow-light band results in a pronounced reduction of the emission lifetime, confirming operation in the high-β regime [2]. At positions of large local chirality, emission becomes strongly directional, with photons deterministically routed into counter-propagating waveguide modes according to the exciton spin state.

Figure 1(a) illustrates the device geometry and the working principle of waveguide-mediated excitation.

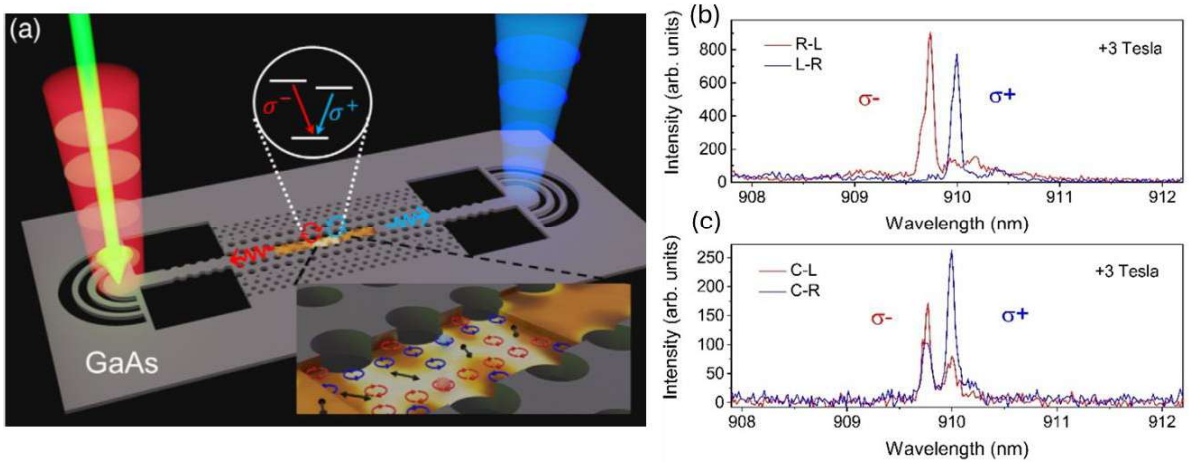

Figure 1. (a) Schematic of chiral emission in a glide-plane waveguide. (b) Enhanced directional contrast under in-plane excitation compared with (c) local excitation.

Photoluminescence measurements obtained via in-plane excitation Fig.1(b) exhibit enhanced directional contrast compared with conventional local excitation Fig.1(c), demonstrating the coexistence of directional absorption and directional emission within the same nanophotonic architecture [3]. Furthermore, for emitters located away from the waveguide centre, we observe a pronounced spectral dependence of the local optical chirality, leading to a controllable variation and in some cases inversion of the directional contrast.

By combining slow-light enhancement, spin-momentum locking, and waveguide-mediated excitation within a photonic device, glide-plane photonic crystal waveguides provide a versatile framework for engineering chiral light-matter interaction with a high degree of control at the single-emitter level. Such capability establishes a pathway toward programmable spin-photon interfaces and scalable quantum photonic circuits based on semiconductor quantum dots.

References

[1] Lodahl P. et al., Nature 541, 473–480 (2017).

[2] Siampour H. et al., npj Quantum Information, 9, 15 (2023).

[3] Germanis S. et al. Optica 12, 1689 (2025).

Coherent superposition of resonantly scattered and emitted single photons from a two-level system

T.V. Shubina[a*], I.V. Krainov[a], A.I. Galimov[a], M.V. Rakhlin[a], and A.A. Toropov[a*]
[a] *Ioffe Institute, 194021 St. Petersburg, Russia*

* Corresponding author: Shubina@beam.ioffe.ru

A typical two-level system - a quantum dot (QD) in a resonator is widely used as a single-photon source for quantum computing and communications. It is generally assumed that for a varying pump pulse area n*π, the maximum amplitude of Rabi oscillations corresponds to a probability of populating the upper level equal to unity for an odd integer n, and the minimum amplitude corresponds to a zero probability for an even n. In fact, for even n, a multiphoton state can emerge from a QD, characterized by a bunch of single photons with a second-order correlation function at zero delay time $g^{(2)}(0)>1$. his phenomenon was attributed to the emission of photon pairs under a single excitation pulse [1]. However, this model could not explain a similar observation for very short pulses and the repeatedly noted absolute necessity of both a charge in the QD and the presence of a resonator.

We investigated the quantum electrodynamics underlying the emergence of such a bunch using a single-photon source created at the Ioffe Institute with a purity and indistinguishability close to unity. It comprises a single InAs/GaAs QD with a positive trion (resident hole) placed in a high-Q micropillar cavity. The measurements were done in a cross-polarization optical scheme with strong laser filtering ~10^{-6}. At pump powers corresponding to odd-π pulses, $g^{(2)}(0)$ is close to zero, whereas at even-π pulse its value can exceed 3. To elucidate the photon nature in the bunch, we measure the Rabi oscillations in photoluminescence (PL), $g^{(2)}(0)$, and PL decay upon the pulse area increased to 6π. Decomposition of the PL decay curves reveals an admixture of resonantly fast scattered laser photons for even π-pulses that is absent for odd π-pulses, which consistent with $g^{(2)}(0)$ oscillation (Fig. 1).

The proposed explanation for this phenomenon takes into account the fact that the laser pulse wave packet contains many photon states (~10^2), which initiate a superposition of Rabi oscillations of varying frequencies and amplitudes. This leads to a nonzero probability of excitation of a trion by a 2π pulse. Since linear polarization is a superposition of left- and right-polarized components; the interaction of the trion spin with one of them leads to a rotation of the polarization angle of resonantly scattered photons, as occurs in the Kerr effect. Due to the presence of a resonator, this nonlinear effect is enhanced by orders of magnitude, resulting in a rotation of several degrees. Thus, despite the strong filtering of the laser light, a coherent superposition of emitted single photons and resonantly scattered laser photons is formed and detected. The developed theoretical model, based on the Jaynes-Cummings approach, describes the observed dependences of Rabi oscillations on the pulse area, as well as $g^{(2)}(0)$, when the QD emission line is detuned in energy relative to the cavity mode [2]. Such coherent multiphoton states with a controlled composition of scattered and emitted photons can be used in quantum technology.

This work is supported by the State Corporation Rosatom within the Quantum Computing Roadmap (contract No. 868/1734-D dated September 22, 2025).

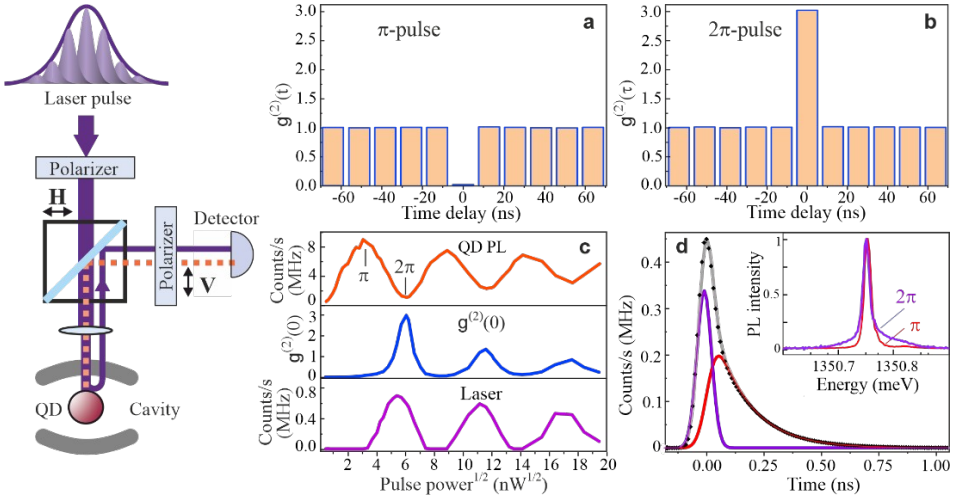

Рис. 1: Cross-polarization measurement scheme with $g^{(2)}(t)$ under excitation (a) by a π-pulse and (b) a 2π-pulse; (c) dependencies of the PL, $g^{(2)}(0)$, and scattered laser light on the pulse power; (d) PL decay curve for 2π excitation decomposed into fast scattered laser light and slow trion emission with the PL lines in the inset.

[1] K.A. Fischer et al. Nature Physics 13, 649 (2017).
[2] I.V. Krainov et al. arXiv:2507.05943v1 [cond-mat.mes-hall] (2025).

Semiconductor–Semimetal Transition in van der Waals Carbyne Crystals

Stella Kavokina, D. Barettin, E. L. Ivchenko and Alexey V. Kavokin

Freestanding van der Waals crystals made of single-atom carbon chains — carbynes — have been recently realized technologically. Here we investigate their electronic and optical properties experimentally, by continuous-wave and timeresolved photoluminescence spectroscopy, and theoretically. Employing a fully three-dimensional tight-binding formalism benchmarked against density functional theory calculations we predict the semimetal-semiconductor transition to occur in van der Waals carbyne crystals composed by the chains of about 42 atoms long. The semiconductor phase is characterized by a hyperbolic van Hove singularity which gives rise to unconventional hyperbolic exciton states. Experimentally, we access the semiconductor phase, where resonant features associated with hyperbolic excitons are clearly visible. The exciton oscillator strength is found to be strongly sensitive to the length of carbon chains: our experiments show that it decreases with the increasing chain length. This tendency, confirmed by the theoretical modeling, manifests the evolution of the hyperbolic exciton state on the way to the semiconductor-semimetal crossover. Our approach accounts for the actual crystalline geometry, including alternating intra-chain hoppings and inter-chain couplings. By fitting tight-binding dispersions to density functional theory data we extract consistent parameters and establish a comprehensive framework for the physics of carbyne crystals. This study paves the way towards efficient band-gap engineering in ultimate one-dimensional carbon crystals.

Telecom C-band single-photon sources based on a semiconductor-dielectric microcavity with a single quantum dot

A.A. Toropov[a*]

[a] *Ioffe Institute, 26 Politekhnicheskaya, St. Petersburg 194021, Russia*

* Corresponding author: toropov@beam.ioffe.ru

Implementation of quantum networks using a well-developed classical optical communications infrastructure imposes a limitation on the operating wavelength of photon sources, which must correspond to the telecommunications C-band (1530-1565 nm) [1]. To obtain deterministic single-photon sources operating in this range, we used an original technological approach, including the formation of an epitaxial metamorphic heterostructure with InAs/InGaAs quantum dots using molecular beam epitaxy (MBE) and the fabrication of a hybrid microresonator with semiconductor and dielectric distributed Bragg reflectors (DBRs) (Fig. 1a). The lower mirror of the microcavity, the $Al_{0.9}Ga_{0.1}As$/GaAs DBR, is formed during the MBE growth of the initial heterostructure, while the upper DBR consists of several pairs of layers of deposited dielectric materials Si/SiO_2. These structures allowed implementation of a resonant coherent mode of pulsed excitation of a single QD, providing, at a pump power corresponding to the first Rabi oscillation (π-pulses), record-high parameters of single-photon emission at a wavelength of 1.554 μm: the purity of single-photon emission of ~97% ($g^{(2)}(0) \sim 0.03$) and a polarized photon emission frequency of 8.8 MHz (in a single-mode optical fiber at a pump frequency of 78.3 MHz), which corresponds to the "first-lens" efficiency of up to 22.8%.

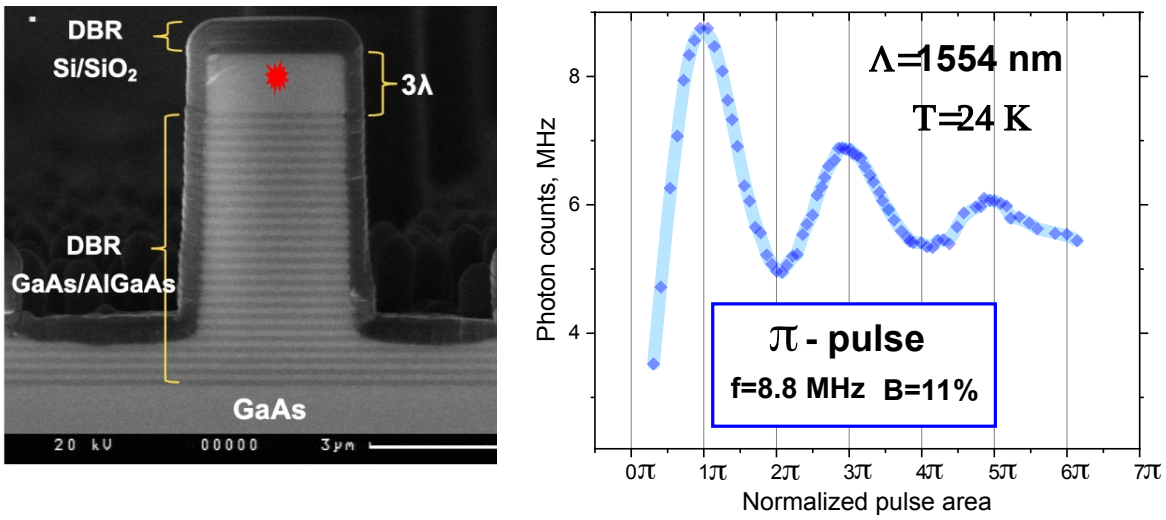

Fig. 1: a) A vertical cross-section of a hybrid cylindrical microresonator, including a lower GaAs/AlGaAs DBR and an upper Si/SiO2 DBR, as well as a metamorphic InGaN buffer layer and an InAs/InGaAs QD in a cavity 3 wavelengths thick. The asterisk schematically indicates the location of the emitting QD. b) Oscillatory dependence of the average photon generation frequency on the normalized area of the pumping laser pulse (in π units). The «end-to-end» efficiency 11% of generating polarized photons in a single-mode optical fiber corresponds to the π-pulse coherent excitation.

The work was supported by Rosatom in the framework of the Roadmap for Quantum computing (Contract №. 868/1734-D dated 22 September 2025).

References

[1] P. Holeva et al, Nanophotonics. **14**, 1729 (2025).

Van der Waals Materials for Advanced Nanophotonics: Perspectives and Challenges

Valentyn S. Volkov[a*]

[a] *Emerging Technologies Research Center, XPANCEO, Internet City, Emmay Tower, Dubai, United Arab Emirates*

* Corresponding author: vsv@xpanceo.com

Van der Waals (vdW) materials are at the core of modern optoelectronics and nanophotonics [1]. Materials with high optical anisotropy are of great importance in technology and science, yet relatively little research attention has been devoted to their giant optical anisotropy. While one of the largest birefringences in the visible and near-infrared intervals (up to 0.8) was reported in the quasi-one-dimensional crystal $BaTiS_3$ [2], anisotropic nanophotonics requires an optical anisotropy of about 1.5 to fully exploit the advantages of anisotropic properties [3-4]. Inspired by this challenge, our focus shifted to two-dimensional materials and their bulk counterparts, vdW materials [5-9]. We demonstrate that the fundamental difference between strong interlayer covalent bonding and weak interlayer van der Waals interaction leads to unprecedented high birefringence. These values exceed 1.5 in the infrared and 3.0 in the visible spectral intervals. Thus, our studies enable a new field of vdW anisotropic nanophotonics. The use of this giant anisotropy leads to next-generation integrated circuits and optical elements. Specifically, we achieved unmatched lateral dimensions for vdW-based waveguides with a footprint of only several tens of nanometers. This provides a unique opportunity to place around 10000 waveguides on a millimeter-scale photonic chip. Such vdW-based photonic integrated circuits can become a decisive platform for an electronic-to-photonic replacement, significantly increasing computer data processing capabilities. The idea behind using vdW materials relies on four distinct advantages. First, they possess a larger optical bandgap compared to conventional high refractive index materials, enabling smaller operation wavelengths without dissipative losses. Second, they exhibit some of the largest refractive indices among known materials. Third, their record-breaking optical anisotropy provides an additional degree of freedom for the design optimization of integrated photonic elements. Finally, the lithography process leaves vdW materials with dangling bonds-free surfaces and atomically sharp edges, resulting in minimal scattering losses and high-intensity nonlinear properties alongside a superior linear response. From a broader perspective, these features are also highly beneficial for countless optical devices beyond on-chip integration, including resonators, dielectric mirrors, and waveplates.

References

[1] G. Ermolaev et al., Nature Communications, 12, 854 (2021).
[2] S. Niu et al., Nature Photonics, 12, 392-396 (2018).
[3] G. Ermolaev et al., Photonics, 9, 744 (2022).
[4] S. Jahani et al., Nature Communications, 9, 1893 (2018)
[5] G. Ermolaev et al., Nature Communications, 12, 854 (2021).
[6] A. Slavich et al., Light: Science & Applications, 13, 68 (2024)
[7] G. Ermolaev et al., arXiv:2505.00920 (2025).
[8] G. Ermolaev et al., arXiv:2509.18866 (2025).
[9] G. Ermolaev et al., Nano Letters (2026).

Chilling Photons in Variable Potentials: From a Two-State System of Light to Quantum Rings

Martin Weitz

Institut für Angewandte Physik, Universität Bonn, Wegelerstr. 8, 53115 Bonn, Germany

Photons in optical microcavities radiatively coupled to a room temperature bath, such as dye molecules or more recently also semiconductor materials, can operate as collective quantum systems of light at near thermal equilibrium conditions, enabling e.g. the observation of photon Bose-Einstein condensates [1-4]. In my Bonn group, we have thermalized photons in a two-mode dye microcavity system at conditions of tuneable chemical potential, demonstrating the elementary statistical mechanical problem of N bosons in a two-level system. To begin with, in a preparatory experiment carried out at pulsed pump conditions, Josephson oscillations between the two quantum states are observed, which verifies the possibility for coherent manipulation. Next, at stationary conditions thermalization of the two-mode system is investigated, arising from the radiative coupling of photons to the dye. Despite that the energetic splitting between the eigenstates is two orders of magnitude below the thermal energy such that at low occupations an almost equal distribution of the modes occupation is observed as expected from Boltzmann statistics, we observe efficient population of the ground state population and saturation of the upper level at high filling [5]. The experiment holds promise for state preparation in quantum technologies as well as for quantum thermodynamics studies. In other work with the dye microcavity system, we have demonstrated the realization a Bose-Einstein condensate of photons in a four-site quantum ring [6]. Photons here macroscopically populate the linear combination of site eigenstates with no phase winding, which is the ground state of the ring lattice.

[1] J. Klaers, J. Schmitt, F. Vewinger, and M. Weitz, Nature **468**, 545 (2010).
[2] See, e.g.: Novel superfluids, Vol. 1, K. H. Bennemann and J. B. Ketterson (eds.) (Oxford University Press, Oxford, 2013).
[3] R. C. Schofield et al., Nature Photonics **18**, 1083 (2024).
[4] M. Pieczarka et al., Nature Photonics **18**, 1090 (2024).
[5] C. Kurtscheid, A. Redmann, F. Vewinger, J. Schmitt, and M. Weitz, Phys. Rev. Lett. **135**, 160406 (2025).
[6] A. Redmann, C. Kurtscheid, N. Wolf, F. Vewinger, J. Schmitt, and M. Weitz, Phys. Rev. Lett. **133**, 093602 (2024).

Toward Epitaxial Growth of Halide Perovskite

Paola De Padova [a], Carlo Ottaviani [a], Bruno Olivieri [a], Filippo Ruggiero [a] and Aldo Di Carlo[a,b*]

[a] *CNR-ISM, Istituto di Struttura della Materia, CNR, via del Fosso del Cavaliere 100, 00133 Rome (Italy)*

[b] *CHOSE-University of Rome Tor Vergata, via del Politecnico 1, 00133 Rome (Italy)*

* Corresponding author: aldo.dicarlo@cnr.it

Molecular beam epitaxy (MBE) is widely regarded as the benchmark technique for layer-by-layer, defect-minimized growth of semiconductor epitaxial films under ultra-high-vacuum (UHV) conditions, typically at base pressures of10^{-10}-10^{-11} mbar. Despite its unparalleled capability to precisely control film composition, thickness, and crystallinity at the atomic scale, its application to halide perovskites has remained relatively limited. In the rapidly evolving field of halide perovskites, however, MBE offers distinctive advantages for fully exploiting the optoelectronic properties of these materials in electronic and photovoltaic devices. In this talk, we will describe the advances performed in the development of MBE growth of halide perovskite, discussing the epitaxial growth mechanisms, structural characteristics, and surface morphology of CsPbBr3 films on various technologically relevant substrates, including Si(111), Si(001), Ag(111), and particularly SiO2-buffered Si(111). We highlight the critical role of an ultra-thin amorphous SiO2 interlayer, introduced by exposure of a clean Si(111)7×7 surface to molecular oxygen, which significantly enhances film quality by mitigating lattice mismatches and facilitating epitaxial growth through a novel "slip-and-stick" mechanism. [1,2] This buffer layer effectively decouples the CsPbBr3 film from the reactive silicon surface, preventing molecular dissociation and facilitating the formation of highly crystalline films. The grown CsPbBr3 perovskite layers were extensively characterized using multiple techniques, including in-situ Auger electron spectroscopy, XRD, RHEED and HAADF-STEM. These analyses revealed uniform stoichiometry throughout the grown films and exceptional crystal quality, with XRD patterns demonstrating sharp reflections indicative of a pure orthorhombic phase with full widths at half maximum (FWHM) as low as 0.035°, comparable to single-crystal silicon standards. Such unprecedented crystallinity points to a significantly reduced defect density and negligible residual stress. HAADF-STEM investigations confirmed the presence of large epitaxial domains spanning several micrometers, each exhibiting uniform alignment of the c-axis perpendicular to the substrate.

These results highlight the strong potential of $CsPbBr_3$ thin films for tandem photovoltaic architectures, especially when integrated with silicon platforms, where they may enable substantial improvements in both device efficiency and operational stability. The approximately 2 nm-thick amorphous SiO_3 interlayer proved crucial in promoting this highly ordered growth mode, as supported by detailed structural modelling and density functional theory (DFT) simulations. [2] The computational results are consistent with the experimental findings and support a “slip-and-stick” diffusion mechanism, in which $CsPbBr_3$ species migrate across the amorphous silica surface with minimal energy barriers, preserving their molecular integrity and enabling uniform layer-by-layer deposition.

Overall, the successful epitaxial growth of $CsPbBr_3$ films by MBE, enabled by a silica buffer layer, underscores the critical importance of substrate engineering and controlled deposition in the fabrication of high-quality perovskite materials. We will also briefly discuss the MBE growth of other lower-bandgap halide perovskites. These findings represent an important step toward the integration of fully inorganic perovskites into robust and efficient optoelectronic devices, next-generation tandem solar cells, and advanced electronic technologies.

References

[1] De Padova, P.; Ottaviani, C.; Olivieri, B.: Ivanov, Y.P.; Divitini, G.;3 Di Carlo, A. The role of SiO2 buffer layer in the molecular beam epitaxy growth of CsPbBr3 perovskite on Si(111), Scientific Reports 2024, 14, 23618.

[2] Tantardini, C.; Argiolas, S.; De Padova, P.; Yakobson, B.I.; Di Carlo, A.; Mattoni, A. Amorphous Silica Interlayer Unlocks Direct Epitaxial Growth of CsPbBr3 on Silicon via Slip-and-Stick Mechanism, J. Phys. Chem. Lett. 2025, 16, 2385−2392.